Chemical Science

ROYAL SOCIETY OF CHEMISTRY

EDGE ARTICLE

View Article Online
View Journal | View Issue

Cite this: *Chem. Sci.*, 2026, **17**, 9582

All publication charges for this article have been paid for by the Royal Society of Chemistry

Received 24th February 2026
Accepted 12th March 2026

DOI: 10.1039/d6sc01577h

rsc.li/chemical-science

Lan enzyme-free construction of lanthionine-bridged macrocyclic phage libraries

Fan Yang, Jiaxi Xiao, Weihang Huang and Jianmin Gao *

Phage display is a powerful technology for discovering macrocyclic peptide ligands. Many phage display-revealed peptide inhibitors comprise disulfide crosslinks, which unfortunately exhibit vulnerability to reduction and proteolysis. Lanthipeptides are a family of ribosomally synthesized peptides that harbor thioether cyclization instead of disulfides. Lanthipeptide libraries have been constructed on phage; however, only with the use of the Lan enzyme that demands specific recognition sequences. Here, we present an enzyme-free strategy for constructing lanthionine-bridged macrocyclic peptide libraries on M13 phage. Our strategy involves selective and reversible masking of the N-terminal cysteine (NCys), followed by Cys-to-Dha conversion and subsequent cyclization upon NCys deprotection. We have specifically optimized the chemistry for each step to allow easy preparation of lanthipeptide libraries. The utility of such libraries is demonstrated by panning against Keap1 as a model protein. To the best of our knowledge, this is the first demonstration of a Lan enzyme-free construction of lanthipeptide libraries on phage, which presents a significant addition to the increasing collection of cyclization chemistries that expand the chemical space of phage display.

Introduction

Phage display is a popular screening technology for discovering peptide probes and inhibitors for various protein targets.[1] Many natural peptides such as neurotoxins and hormones are stabilized by intramolecular disulfide bonds.[2,3] Phage libraries of disulfide-cyclized peptides have also been increasingly adopted for probe and inhibitor discovery.[4,5] Unfortunately, disulfide bonds are unstable in reducing environments and also prone to disulfide exchange, which imposes a major limitation on the use of disulfide-cyclized peptides as therapeutics.[6,7] By contrast, thioether bridges are free of these problems, offering a non-reducible, non-exchangeable alternative to disulfides.[8–11] Nature provides an inspiring example of this crosslink with lanthipeptides, which are members of ribosomally synthesized and post-translationally modified peptides (RiPPs). For lanthipeptide biosynthesis, serine or threonine residues are enzymatically dehydrated to dehydroalanine (Dha) or dehydrobutyrine (Dhb), which then undergo cyclase-mediated intramolecular Michael addition to form the (methyl)lanthionine linkage. Such thioether-bridged peptides have been shown to maintain stability and bioactive conformation in many cases.[11–15]

Lanthipeptide libraries have been developed on both phage and yeast display platforms by harnessing enzymes for lanthipeptide biosynthesis (Fig. 1A).[16–18] However these enzymatic approaches encounter several limitations: displaying peptides on the N-terminus of pIII required Tat export as well as exogenous leader peptide cleavage,[17] while an attempt for C-terminal display afforded low display valency on pIII (0.3 copies per virion), which diminishes the chance of enriching weak binders in early rounds.[18] Furthermore, the enzyme processing steps impose sequence biases: even the broadly tolerant LanM and LanBC systems exhibit kinetically preferred sequences for dehydration and cyclization.[19,20] Chemical installation of a lanthionine bridge necessitates the use of a pre-made lanthionine in solid phase peptide synthesis (Fig. 1B) or carefully designed nonnatural amino acids, which cannot be extended to genetically encoded peptide libraries.[21–23]

We report herein a biocompatible and enzyme-free route to install lanthionine bridges directly on phage display libraries (Fig. 1C). With a CX_nC peptide on phage, the N-terminal cysteine is transiently masked as a thiazolidine, and then the internal cysteine is converted to Dha *via* alkylation–elimination under mild conditions. Unmasking of the N-terminal cysteine triggers intramolecular thia-Michael addition to forge a non-reducible thioether bond. We demonstrate the applicability of this protocol with model peptides, phage coat proteins, and bacteriophage. Importantly, this three-step protocol minimally compromises phage infectivity to give libraries that can be used in standard panning workflows. As a case study, we screened a lanthionine-bridged CX_7C library against Keap1, which yielded Keap1–Nrf2 inhibitors of nanomolar potency.

Results and discussion

Dehydroalanine (Dha) installation

To create lanthipeptide libraries, our first objective was to establish a phage-compatible method for installing

Department of Chemistry, Merkert Chemistry Center, Boston College, Chestnut Hill, MA 02467, USA. E-mail: jianmin.gao@bc.edu

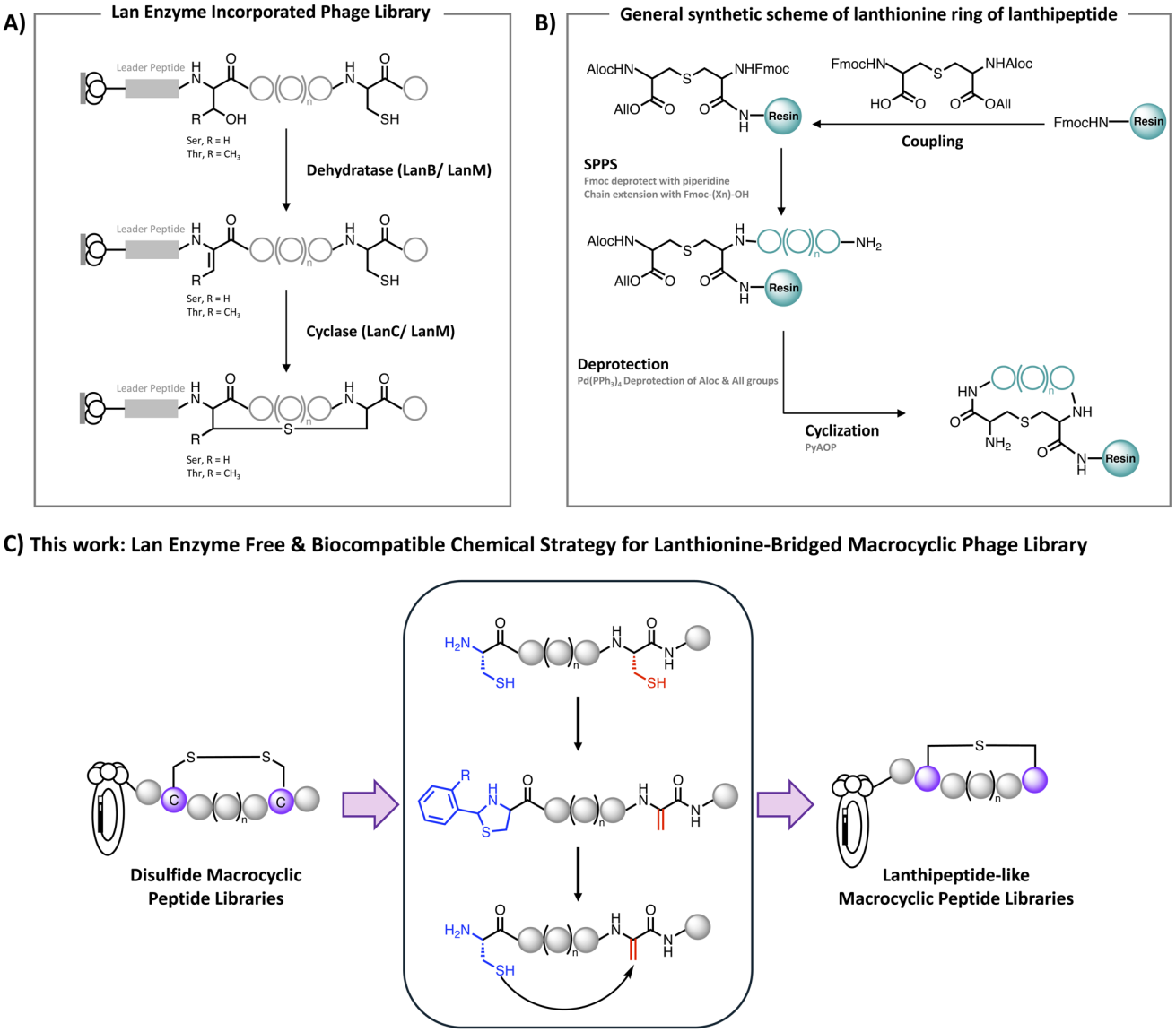

Fig. 1 Strategies for generating lanthionine-cyclized peptide libraries. (A) Phage or yeast display of lanthipeptide libraries requires co-expression of Lan enzymes, as well as fixed sequences for leader peptides and proximal regions of the key Ser/Thr/Cys residue. (B) Chemical lanthipeptide synthesis typically uses a premade lanthionine in solid phase peptide synthesis, which cannot be extended to genetically encoded libraries. (C) Our three-step thioether macrocyclization strategy enables facile construction and screening of lanthipeptide phage libraries.

dehydroalanine (Dha), a prerequisite for forging a lanthionine bridge on displayed peptides. Several reports describe chemical strategies for site-specific conversion of a native residue (cysteine or serine) to Dha on proteins to study ubiquitination or to generate antibody–drug conjugates.[24–26] These prior reports underscore the utility of Dha as a versatile handle for bioconjugation. However, these Dha conversion methods have not been successfully applied to modifying phage-displayed proteins or peptides, where preserving phage infectivity is paramount. To install Dha on phage, we evaluated three methods for Cys-to-Dha conversion on a model peptide to begin with. These methods utilize mesitylenesulfonylhydroxylamine (MSH),[24] 2,5-dibromohexanediamide (DBHDA),[27] and methyl-2,5-dibromopentanoate (MDBP),[28] respectively, to induce desulfurization (Fig. 2A). All three reagents enabled clean conversion of the cysteine residue on the model peptide to Dha, as quantified by LC-MS analysis, albeit with distinct reaction time and reagent concentration (Fig. S6–S8 and Schemes S3–S5). Encouraged by these results, we quantitatively assessed the impact of each reagent on phage viability through titering. Treatment with MSH proved profoundly detrimental, resulting in a 10^6 fold reduction in viable phage titer compared to the non-treated control (Fig. 2B). This massive loss of infectivity is likely due to the off-target reactivity of MSH on the virion surface. In addition to cysteines, MSH can react with other nucleophiles, including imidazoles (His), carboxylates (Asp/Glu), and amines (Lys/N-terminus), leading to nonselective N/S-amination or oxidative/deamination events.[29] Consequently,

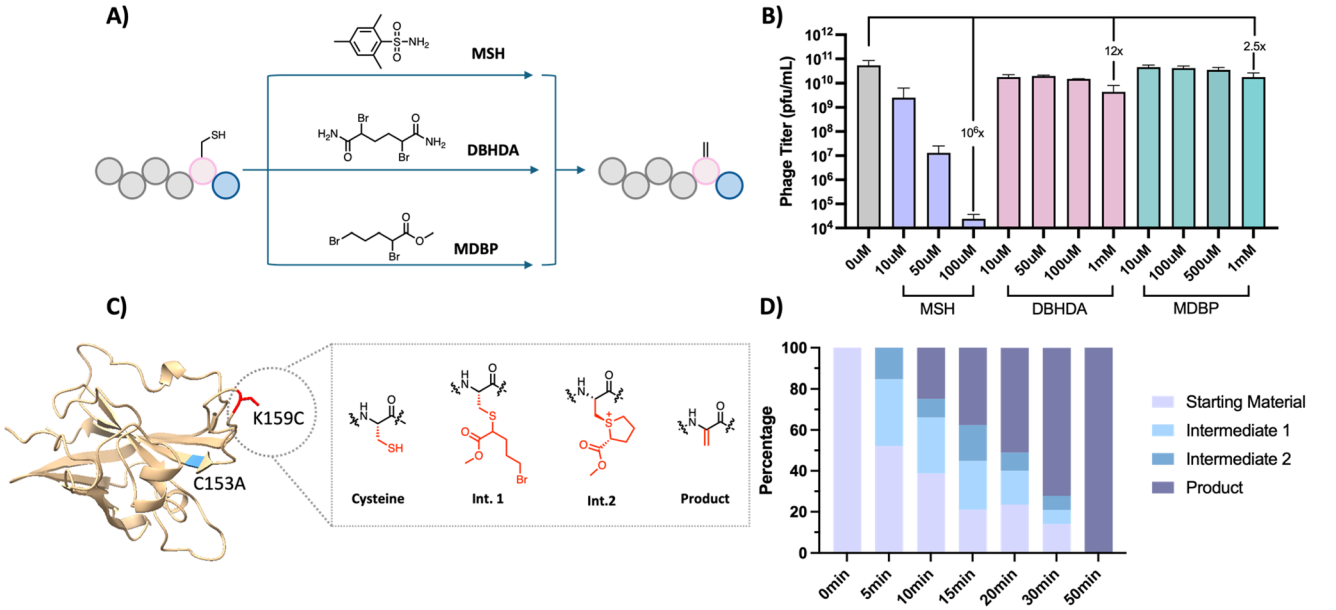

Fig. 2 Chemically induced Cys-to-Dha conversion. (A) Dha conversion from an internal cysteine on a model peptide. (B) Phage infectivity change encountered by the three Dha conversion strategies. (C) Dha conversion from an internal cysteine on a model protein of SrtA (C153A and K159C) by MDBP. (D) Reaction kinetics of the MDBP-induced Dha formation.

MSH was excluded from further exploration. DBHDA was tolerated but suboptimal, incurring a substantial (12-fold) diminution in phage titer. MDBP was much better tolerated: under conditions that afforded quantitative Dha conversion, the loss in phage infectivity was just 2.5 fold, which makes MDBP the best reagent for inducing Cys-to-Dha conversions.

Encouraged by its minimal toxicity, we decided to better understand the MDBP-induced Dha formation in the context of proteins, which present a complex mixture of nucleophiles. Specifically, we engineered a sortase A (SrtA) variant, which has its catalytic cysteine mutated to alanine (C153A) and a solvent-accessible lysine mutated into cysteine (K159C). Kinetic analysis of the SrtA modification monitored by LC-MS revealed rapid Dha product accumulation upon treatment with MDBP (Fig. 2D and S19–S26). Interestingly, these kinetic studies revealed two key intermediates: the initial thioether conjugate (Intermediate 1) and a subsequent sulfonium salt (Intermediate 2), which undergo elimination to form Dha (Fig. 2C). This delineated reaction pathway confirms the alkylation–elimination mechanism and suggests efficient progression through both steps. For comparison, DBHDA demonstrated slower kinetics and less complete conversion under identical conditions (Fig. S9–S18). Furthermore, while the initial thioether intermediate (Intermediate 1) was detectable, the subsequent sulfonium salt intermediate (Intermediate 2) was conspicuously absent. We rationalize that the bulkier diamide scaffold of DBHDA introduces significant steric encumbrance, which likely hinders the intramolecular cyclization required to form the strained sulfonium ring, thereby slowing the elimination step. Overall, MDBP exhibited rapid and quantitative conversion kinetics on both peptide and protein substrates, which, together with its excellent phage compatibility, makes it uniquely suitable for chemical modification of phage libraries.

Lanthionine cyclization

With a phage-compatible method for Dha installation in place, we next optimized a three-step strategy to achieve lanthionine macrocyclization on phage. Our strategy builds on readily accessible CX_nC phage libraries. The internal cysteine is converted to Dha while the N-terminal cysteine (NCys) is preserved for subsequent cyclization. Specifically, we take advantage of the differential reactivity of NCys to protect it using an aldehyde that reacts with NCys to form a quasi-stable thiazolidine.[30–32] With NCys protected, the internal cysteine can be converted to Dha using MDBP and optimized conditions described above. Subsequent deprotection of the NCys elicits macrocyclization to give a thioether linkage (Fig. 3A). We first tested this protocol with model peptides (Fig. 3B). Initial screening of various aldehyde reagents, including 2-formylphenylboronic acid (FPBA), salicylaldehyde (SA), and benzaldehyde (BA), revealed FPBA as the most effective NCys masking reagent – it afforded quantitative protection of the N-Cys residue within 30 minutes under mild aqueous conditions (pH 7.4), without detectable side reactions (Fig. S28, S33 and S38).[31–33] The FPBA protected peptide was then subjected to MDBP treatment, which elicited >90% Cys-to-Dha conversion, while the protected NCys remained entirely intact (Fig. S39). The thiazolidine deprotection and subsequent cyclization were triggered by simply raising the pH, yielding a lanthionine-bridged macrocycle in quantitative yield. Importantly, this protocol proved sequence-tolerant, giving high-yield lanthionine macrocyclization across multiple model peptides differing in NCys–Dha spacing and side-chain composition (Schemes S18–22). To confirm the postulated lanthionine formation, we synthesized two lanthipeptides using a pre-made lanthionine as a building block in solid phase peptide synthesis (SPPS) (Schemes S21 and 22).

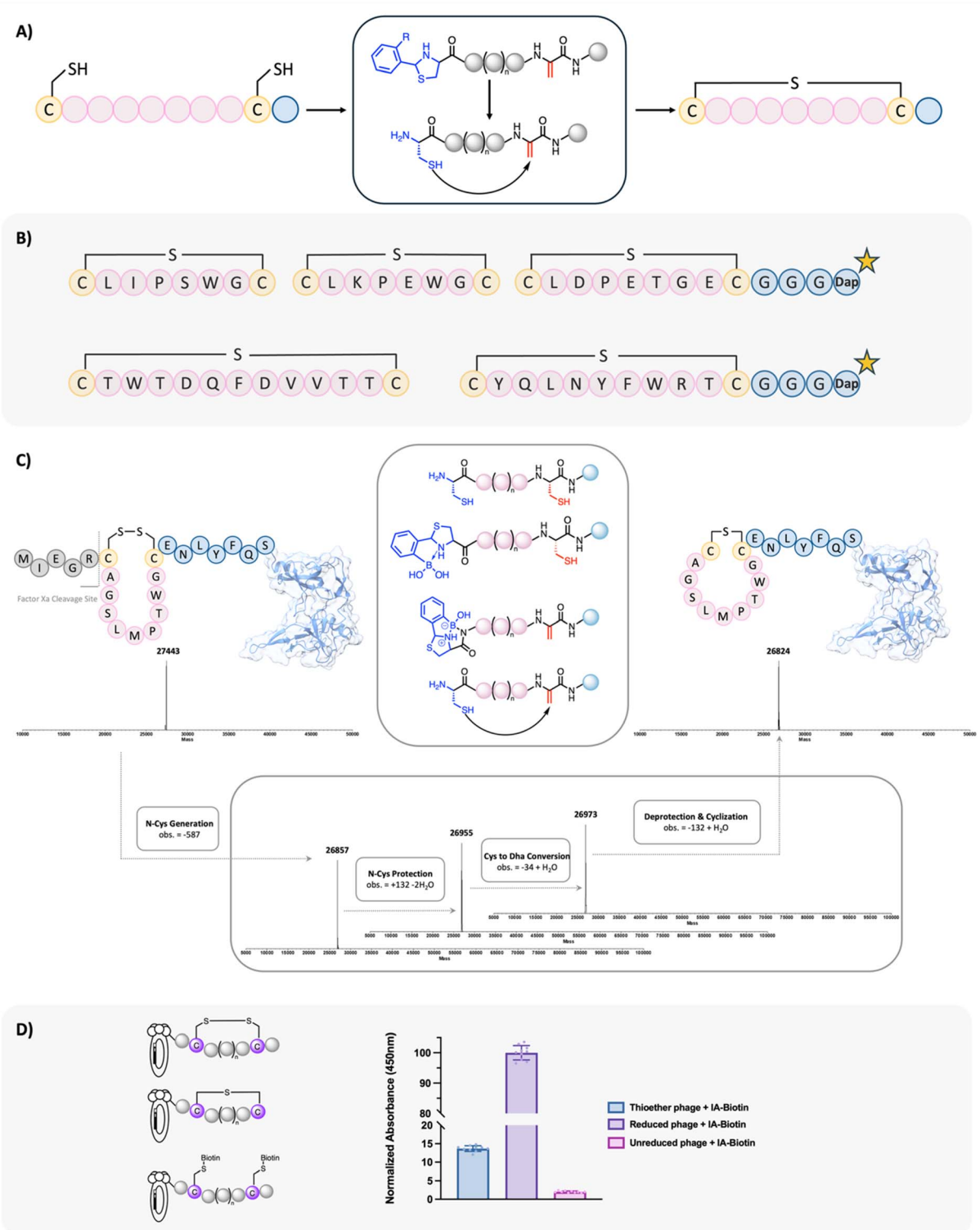

Fig. 3 Enzyme-free lanthipeptide synthesis. (A) Schematic of the lanthionine-bridged peptide macrocycle formed from NCys and Dha *via* intramolecular Michael addition. (B) Model peptides with different sequences and loop sizes used to evaluate the generality of our thioether macrocyclization protocol. Corresponding LC-MS traces are detailed in the SI. (C) Lanthipeptide synthesis with a precursor peptide-pIII fusion. Sequence of treatments: (1) factor Xa cleavage; TCEP reduction (1 mM, ammonium bicarbonate, pH 8.0); (2) FPBA (1 mM, PBS, pH 7.4, 30 min, r.t.); (3) MDBP (1 mM, sodium phosphate, pH 8.5, 37 °C, 1 h); (4) basic incubation (pH 10, 37 °C, 1 h) for NCys deprotection/cyclization. Stepwise mass-spec data are shown to reveal a clean and efficient conversion. (D) Assessing the efficiency of thioether macrocyclization of a CX_7C library *via* a phage capture assay. Assayed groups include: non-reduced phage library labeled by IA-biotin (right), TCEP-reduced phage library labeled by IA-biotin (middle), and thioether phage library treated with TCEP and then IA-biotin (left).

Then the lanthipeptides synthesized *via* SPPS (positive controls) and those made through our NCys–Dha cyclization were comparatively analyzed *via* LC-MS. The results show that our NCys–Dha cyclized peptides and their corresponding positive controls coelute as a single peak on LC-MS and exhibit identical mass-spec signatures. We acknowledge that our NCys–Dha cyclization protocol may produce a pair of diastereomeric peptides with mixed stereochemistry at the Dha position. While more detailed stereochemical characterization is warranted for future studies, our results presented above showcase a robust, stepwise yet streamlined chemical method that achieves site-specific lanthionine bridging with no need for a Lan enzyme.

We further extended the workflow to a protein, specifically to a recombinant pIII of the M13 phage that has the peptide CAGSLMPTWGC fused at its N terminus (Fig. S52). The recombinant pIII fusion was first reduced with TCEP in ammonium bicarbonate buffer (pH 8.0), and then processed sequentially: (i) FPBA (1 mM) in PBS (pH 7.4, 30 min, r.t.) to form the NCys thiazolidine; (ii) MDBP (1 mM) in sodium phosphate buffer (pH 8.5, 1 h, 37 °C) to convert the internal Cys to Dha; and (iii) NCys deprotection and spontaneous cyclization under basic conditions (pH 10, 1 h, 37 °C). Stepwise LC-MS monitoring confirmed each transformation and showed that the lanthionine-bridged, macrocyclized pIII protein was the major product (Fig. 3C and S53–S55). To probe the applicability of our lanthionine cyclization protocol to phage, we constructed a CX_7C phage library with a factor Xa cleavage site immediately upstream of the CX_7C insert.[34] Factor Xa cleavage followed by TCEP reduction prepares the phage library for the three-step macrocyclization. We next evaluated the efficiency of on-phage lanthionine cyclization using a streptavidin-capture ELISA, which was developed by Derda and coworkers to report iodoacetamide-biotin (IA-biotin) labeling of accessible thiols.[35] As positive controls, we treated the reduced CX_7C phage library with IA-biotin and subjected to streptavidin pulldown with streptavidin-coated wells (Fig. 3D) and streptavidin-coated beads (Fig. S60). Efficient phage pulldown was observed for both cases. The phage library without TCEP reduction served as a negative control, which encountered little pulldown in the ELISA assay performed in the 96-well plate (Fig. 3D). Then, the CX_7C library was subjected to the three-step protocol for lanthionine modification. The resulting, putative thioether library was subjected to TCEP reduction and then pulldown with streptavidin-coated wells. This experiment gave a low percentage of (<15%) pulldown readout, indicating an efficient thioether formation that leaves few disulfide phage around.

To gain a full picture of our lanthionine cyclization protocol, we titered the phage population after each step of the phage modification protocol. A small extent of phage loss (<5-fold, Fig. S56) was observed for all steps, accumulating to ~50 fold reduction in phage population throughout the whole modification protocol. We note that the phage loss is not necessarily caused by the toxicity of the chemical reagents used. Instead, there are a number of phage precipitation steps throughout the phage modification protocol, which inevitably cause mechanical losses of phage. Importantly, we performed amplicon sequencing of the library before and after the lanthionine cyclization, the results of which suggest no clear sequence bias in the phage loss. Specifically, we treated the naïve CX_7C library with the lanthionine cyclization protocol and then subjected the library to reduction and TCEP pulldown to remove any remaining disulfide-cyclized phage. The resulting thioether library and the naïve library were submitted for amplicon sequencing (Fig. S57). The amplicon sequencing reads (>100 000) of both libraries revealed no more than 5 copies of any unique sequence (Table S3). In fact, for the naïve library, 97.4% of the amplicon reads represent unique sequences, and an essentially identical number (97.8%) was obtained for the thioether library. We further analyzed the amino acid composition of each randomized position of the library peptides. Both the naïve library and the thioether library give a dispersed distribution with every amino acid present at significant percentages at every position, again indicating a diverse sequence space for both libraries (Fig. S58). There is no discernible difference in amino acid composition patterns between the two libraries, indicating that no significant sequence bias was introduced by our lanthionine cyclization protocol. Lending further evidence to this conclusion, we randomly isolated ten phage colonies, which were subjected to lanthionine cyclization and then phage titering (Fig. S59). The ten colonies afforded comparable phage counts, again indicating a lack of sequence bias in our lanthionine cyclization protocol.

Lanthipeptide library screening to identify protein–protein interaction inhibitors

To assess the utility of our lanthionine-bridged phage library, we conducted phage selections against Keap1 as a case study (Fig. 4A). Keap1 is the substrate adaptor of a CUL3 E3 ubiquitin ligase that targets Nrf2 for ubiquitination and proteasomal degradation.[36,37] Disrupting the Keap1–Nrf2 interaction stabilizes Nrf2, drives its nuclear accumulation, and activates the antioxidant response element, a pathway of broad interest in diseases marked by oxidative or electrophilic stress.[38–40] Not surprisingly, inhibition of the Keap1–Nrf2 interaction has attracted significant attention in recent literature.[34,41] We constructed a CX_7C phage library with a generic sequence of HAtag-IEGRCX_7C-GGGS-pIII. This library was converted into a lanthipeptide library using the abovementioned protocol and screened against Keap1. For phage panning, Keap1 was recombinantly expressed with an N-terminal His-tag and then chemically biotinylated using biotin-NHS. The biotinylated Keap1 protein was immobilized on streptavidin-coated magnetic beads for phage selections. The enrichment of the Keap1-binding phage was monitored by titering the output population in each round, which was further analyzed *via* next generation sequencing (NGS). Four rounds of selection were carried out (Fig. 4B), including a negative selection against the streptavidin beads for Round 1 (R1). We observed a steady increase in output phage count. The NGS results revealed a clear winner sequence, dubbed FK1, which constitutes 93% of the R4 output population. Interestingly, a closer examination of the FK1 abundance in our NGS data revealed a consistent enrichment across the rounds of selections. Specifically, FK1 was seen

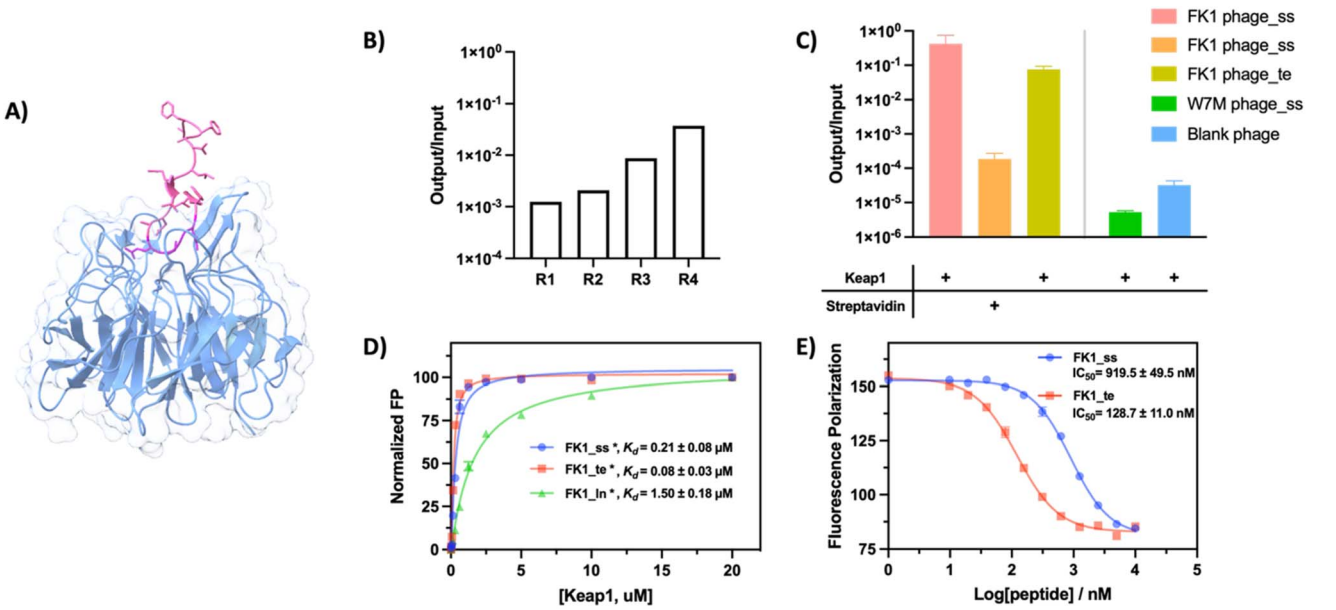

Fig. 4 Lanthipeptide phage library screening against Keap1 yields a nanomolar inhibitor. (A) Crystal structure of the Keap1 Kelch domain in complex with the Nrf2 peptide (PDB 2FLU). (B) Output/input ratio of phage panning indicating gradual enrichment of Keap1 binding clones. (C) Phage retention by Keap1 or streptavidin coated beads. (D) Fluorescence polarization-based binding profiles of various FK1 peptides towards the target protein Keap1. *: FAM labelled peptide. (E) FK1 peptides' inhibition of Keap1–Nrf2 interaction; a fluorophore labeled peptide (Fam-bAla-DEETGEF) was used as a Nrf2 mimic. Each data point in (D) and (E) represents the mean value of three independent measurements.

only once (out of >233 000 reads in amplicon sequencing) in the round 1 output population, and its population percentage increased to 0.2% in R2, 56% in R3 and then 93% in R4 (Fig. S61). Similar to what we did with the naïve library, we analyzed the amino acid composition at each randomized position during the phage panning process. As expected, clear sequence convergence was seen in the plotted results of amino acid compositions (Fig. S62).

To validate the enriched FK1 as a specific Keap1 binder, we first validated the FK1 phage by a phage-retention assay, comparing the retention of the lanthionine-bridged FK1 phage with its disulfide-cyclized precursor on bead-immobilized Keap1. The two phage variants showed comparably high retention, indicating that installing the lanthionine staple preserves target binding and phage infectivity relative to the disulfide precursor. As negative controls, a blank phage and a sortase-binding phage W7M showed no retention on Keap1 (Fig. 4C). Furthermore, both FK1 variants failed to bind streptavidin beads alone. Collectively, these results demonstrate that the lanthionine-bridged FK1 phage is indeed enriched through specific interactions with Keap1. We next chemically synthesized fluorescein-labeled FK1 peptides in linear, disulfide-cyclized, and lanthionine-bridged formats, with fluorescein installed on a C-terminal diaminopropionic acid (Dap) residue preceded by a –GGG– linker (Fig. S63–S68). The binding affinity of these peptide variants to Keap1 was quantified by fluorescence polarization (FP). Briefly, a fixed concentration of peptide was incubated with serial dilutions of Keap1. FP values were recorded using a fluorescence plate reader and plotted against protein concentration to generate a binding curve. K_d values were extracted *via* curve fitting (Fig. 4D and S76). Satisfyingly, the thioether-bridged FK1 (FK1_te) was found to exhibit nanomolar affinity (K_d = 0.08 μM), whereas the linear peptide was ~20 times weaker, with a K_d of 1.5 μM. The disulfide-cyclized FK1 (FK1_ss) also gave a slightly higher K_d compared to the thioether variant. To ensure the validity of these binding data, we resorted to a flow cytometry-based method for assessing Keap1 binding of peptides. Specifically, Keap1 coated magnetic beads were treated with fluorophore-labeled peptides at varied concentrations. The extent of peptide binding was quantified by flow cytometry readout of bead fluorescence, which was then plotted against peptide concentration (Fig. S77). Curve fitting yielded similar K_d values as obtained from the FP assay. Again, the thioether peptide showed close to 20 times stronger binding affinity than the linear comparison.

To assess the chemical stability of the thioether linkage, we evaluated the susceptibility of FK1_te to ring-opening under both reducing and acylating conditions. FK1_te was incubated with 5 mM iodoacetamide (IA) in ammonium bicarbonate buffer (pH 8.0) at room temperature, and aliquots were collected over time for LC-MS analysis (Fig. S72). No IA adducts were detected throughout the assay window, indicating negligible ring opening under strongly alkylating conditions. Additionally, FK1_te was treated with 1 mM TCEP under the same buffer conditions (Fig. S69). Similarly, no mass shift or linearized peptide species were observed, confirming that the thioether staple is chemically stable and resistant to both nucleophilic reduction and acylation. To assess thermal/proteolytic stability, FK1_te and FK1_ss control were incubated in human serum at 37 °C and their integrity was analyzed by LC-MS over time (Fig. S73–S75). The lanthionine-bridged peptide showed markedly greater stability, with ~60% intact peptides remaining at the 5 h time point, in contrast to the disulfide

control, which had <20% remaining. Finally, the FK1 peptides were assessed for their inhibitory activity of Keap1–Nrf2 binding under reducing conditions (with the addition of GSH). Briefly, the FK1 peptides without a fluorophore label were titrated into a pre-formed complex of Keap1 with a fluorescently labeled Nrf2. As expected, the competition assay revealed an IC_{50} of 128 nM for FK1_te, ~8 times lower than that of FK1_ss. Note that the IC_{50} of FK1_ss is approaching the K_d of FK1_ln, consistent with the disulfide peptide undergoing reduction to give a linear peptide under the experimental conditions (Fig. 4E). The contrast of these two peptides highlights the advantage of the thioether-cyclized peptide macrocycles.

Conclusion

We have established a Lan enzyme-free strategy to construct lanthipeptide libraries on M13 phage. The workflow proceeds sequentially with reversible NCys masking as a thiazolidine, Cys-to-Dha conversion, and one-pot deprotection/intramolecular thia-Michael cyclization. This three-step protocol proved tolerant of various peptide sequences, minimally compromised phage infectivity, and delivered highly efficient disulfide-to-thioether conversions on model peptides, proteins as well as bacteriophage. Applying this protocol to phage display, we have successfully constructed a CX_7C thioether library, screening of which readily revealed a nanomolar peptide inhibitor of the Keap1–Nrf2 interaction. Importantly, in comparison to the disulfide precursor, the thioether peptide inhibitor show superior potency under reducing conditions, highlighting the intrinsic advantage of the thioether-bridged peptide macrocycles. Conceptually, this strategy provides a facile replacement for disulfide-cyclized peptides: libraries with the design of CX_nC can be retrofitted to their thioether-stapled counterparts without altering selection workflows. Practically, it expands the accessible chemical space for phage display by coupling precise, site-selective Dha chemistry to infectivity-preserving macrocyclization. Beyond the Keap1 benchmark, we envision that the platform is broadly applicable to challenging proteins and especially suited for intracellular PPIs, which demand reduction-safe inhibitors.

Author contributions

F. Yang: conceptualization; methodology; investigation; formal analysis; visualization; writing – original draft; writing – review & editing. J. Xiao: investigation. W. Huang: investigation. J. Gao: conceptualization; writing – review & editing; supervision; funding acquisition.

Conflicts of interest

There are no conflicts to declare.

Data availability

The data supporting this article have been included as part of the supplementary information (SI). Supplementary information: Fig. S1–S77, detailed characterization data of peptides and proteins and their reactions; Tables S1–S2: LC-MS conditions; S3, enriched peptide sequences; Section 7, NMR spectra of synthetic compounds. See DOI: https://doi.org/10.1039/d6sc01577h.

Acknowledgements

The financial support of this work is provided by the U.S. National Institutes of Health through grant GM152005 (to J. G.).

References

1 G. P. Smith and V. A. Petrenko, Phage Display, *Chem. Rev.*, 1997, **97**(2), 391–410, DOI: 10.1021/cr960065d.
2 R. I. Lehrer, A. K. Lichtenstein and T. Ganz, Defensins: Antimicrobial and Cytotoxic Peptides of Mammalian Cells, *Annu. Rev. Immunol.*, 1993, **11**, 105–128, DOI: 10.1146/annurev.iy.11.040193.000541.
3 C. Avitabile, R. Capparelli, M. M. Rigano, A. Fulgione, A. Barone, C. Pedone and A. Romanelli, Antimicrobial Peptides from Plants: Stabilization of the γ Core of a Tomato Defensin by Intramolecular Disulfide Bond, *J. Pept. Sci.*, 2013, **19**(4), 240–245, DOI: 10.1002/psc.2479.
4 S. Chen, I. Rentero Rebollo, S. A. Buth, J. Morales-Sanfrutos, J. Touati, P. G. Leiman and C. Heinis, Bicyclic Peptide Ligands Pulled out of Cysteine-Rich Peptide Libraries, *J. Am. Chem. Soc.*, 2013, **135**(17), 6562–6569, DOI: 10.1021/ja400461h.
5 M. Zha, P. Lin, H. Yao, Y. Zhao and C. Wu, A Phage Display-Based Strategy for the de Novo Creation of Disulfide-Constrained and Isomer-Free Bicyclic Peptide Affinity Reagents, *Chem. Commun.*, 2018, **54**(32), 4029–4032, DOI: 10.1039/C7CC09142G.
6 A. Gori, P. Gagni and S. Rinaldi, Disulfide Bond Mimetics: Strategies and Challenges, *Chemistry*, 2017, **23**(60), 14987–14995, DOI: 10.1002/chem.201703199.
7 Y. Gu, J. A. Iannuzzelli and R. Fasan, MOrPH-PhD: A Phage Display System for the Functional Selection of Genetically Encoded Macrocyclic Peptides, *Methods Mol. Biol.*, 2022, **2371**, 261–286, DOI: 10.1007/978-1-0716-1689-5_14.
8 J. Lindgren and A. Eriksson Karlström, Intramolecular Thioether Crosslinking of Therapeutic Proteins to Increase Proteolytic Stability, *ChemBioChem*, 2014, **15**(14), 2132–2138, DOI: 10.1002/cbic.201400002.
9 K. Pulka-Ziach, V. Pavet, N. Chekkat, K. Estieu-Gionnet, R. Rohac, M.-C. Lechner, C. R. Smulski, G. Zeder-Lutz, D. Altschuh, H. Gronemeyer, S. Fournel, B. Odaert and G. Guichard, Thioether Analogues of Disulfide-Bridged Cyclic Peptides Targeting Death Receptor 5: Conformational Analysis, Dimerisation and Consequences for Receptor Activation, *ChemBioChem*, 2015, **16**(2), 293–301, DOI: 10.1002/cbic.201402485.
10 H. Xiang, L. Bai, X. Zhang, T. Dan, P. Cheng, X. Yang, H. Ai, K. Li and X. Lei, A Facile Strategy for the Construction of a Phage Display Cyclic Peptide Library for the Selection of

Functional Macrocycles, *Chem. Sci.*, 2024, **15**(30), 11847–11855, DOI: 10.1039/D4SC03207A.

11 W. T. P. Darling, L. H. E. Wieske, D. T. Cook, A. E. Aliev, L. Caron, E. J. Humphrys, A. M. Figueiredo, D. F. Hansen, M. Erdélyi and A. B. Tabor, The Influence of Disulfide, Thioacetal and Lanthionine-Bridges on the Conformation of a Macrocyclic Peptide, *Chem.–Eur. J.*, 2024, **30**(50), e202401654, DOI: 10.1002/chem.202401654.

12 D. P. Teufel, G. Bennett, H. Harrison, K. van Rietschoten, S. Pavan, C. Stace, F. Le Floch, T. Van Bergen, E. Vermassen, P. Barbeaux, T.-T. Hu, J. H. M. Feyen and M. Vanhove, Stable and Long-Lasting, Novel Bicyclic Peptide Plasma Kallikrein Inhibitors for the Treatment of Diabetic Macular Edema, *J. Med. Chem.*, 2018, **61**(7), 2823–2836, DOI: 10.1021/acs.jmedchem.7b01625.

13 C. Gowland, P. Berry, J. Errington, P. Jeffrey, G. Bennett, L. Godfrey, M. Pittman, A. Niewiarowski, S. N. Symeonides and G. J. Veal, Development of a Lc–Ms/Ms Method for the Quantification of Toxic Payload Dm1 Cleaved from Bt1718 in a Phase I Study, *Bioanalysis*, 2021, **13**(2), 101–113, DOI: 10.4155/bio-2020-0256.

14 M. Montalbán-López, T. A. Scott, S. Ramesh, I. R. Rahman, A. J. van Heel, J. H. Viel, V. Bandarian, E. Dittmann, O. Genilloud, Y. Goto, M. J. Grande Burgos, C. Hill, S. Kim, J. Koehnke, J. A. Latham, A. J. Link, B. Martínez, S. K. Nair, Y. Nicolet, S. Rebuffat, H.-G. Sahl, D. Sareen, E. W. Schmidt, L. Schmitt, K. Severinov, R. D. Süssmuth, A. W. Truman, H. Wang, J.-K. Weng, G. P. van Wezel, Q. Zhang, J. Zhong, J. Piel, D. A. Mitchell, O. P. Kuipers and W. A. van der Donk, New Developments in RiPP Discovery, Enzymology and Engineering, *Nat. Prod. Rep.*, 2021, **38**(1), 130–239, DOI: 10.1039/d0np00027b.

15 F.-J. Chen, N. Pinnette, F. Yang and J. Gao, A Cysteine-Directed Proximity-Driven Crosslinking Method for Native Peptide Bicyclization, *Angew. Chem.*, 2023, **135**(31), e202306813, DOI: 10.1002/ange.202306813.

16 X. Yang, K. R. Lennard, C. He, M. C. Walker, A. T. Ball, C. Doigneaux, A. Tavassoli and W. A. van der Donk, A Lanthipeptide Library Used to Identify a Protein–Protein Interaction Inhibitor, *Nat. Chem. Biol.*, 2018, **14**(4), 375–380, DOI: 10.1038/s41589-018-0008-5.

17 K. J. Hetrick, M. C. Walker and W. A. van der Donk, Development and Application of Yeast and Phage Display of Diverse Lanthipeptides, *ACS Cent. Sci.*, 2018, **4**(4), 458–467, DOI: 10.1021/acscentsci.7b00581.

18 J. H. Urban, M. A. Moosmeier, T. Aumüller, M. Thein, T. Bosma, R. Rink, K. Groth, M. Zulley, K. Siegers, K. Tissot, G. N. Moll and J. Prassler, Phage Display and Selection of Lanthipeptides on the Carboxy-Terminus of the Gene-3 Minor Coat Protein, *Nat. Commun.*, 2017, **8**(1), 1500, DOI: 10.1038/s41467-017-01413-7.

19 P. G. Arnison, M. J. Bibb, G. Bierbaum, A. A. Bowers, T. S. Bugni, G. Bulaj, J. A. Camarero, D. J. Campopiano, G. L. Challis, J. Clardy, P. D. Cotter, D. J. Craik, M. Dawson, E. Dittmann, S. Donadio, P. C. Dorrestein, K.-D. Entian, M. A. Fischbach, J. S. Garavelli, U. Göransson, C. W. Gruber, D. H. Haft, T. K. Hemscheidt, C. Hertweck, C. Hill, A. R. Horswill, M. Jaspars, W. L. Kelly, J. P. Klinman, O. P. Kuipers, A. J. Link, W. Liu, M. A. Marahiel, D. A. Mitchell, G. N. Moll, B. S. Moore, R. Müller, S. K. Nair, I. F. Nes, G. E. Norris, B. M. Olivera, H. Onaka, M. L. Patchett, J. Piel, M. J. T. Reaney, S. Rebuffat, R. P. Ross, H.-G. Sahl, E. W. Schmidt, M. E. Selsted, K. Severinov, B. Shen, K. Sivonen, L. Smith, T. Stein, R. D. Süssmuth, J. R. Tagg, G.-L. Tang, A. W. Truman, J. C. Vederas, C. T. Walsh, J. D. Walton, S. C. Wenzel, J. M. Willey and W. A. van der Donk, Ribosomally Synthesized and Post-Translationally Modified Peptide Natural Products: Overview and Recommendations for a Universal Nomenclature, *Nat. Prod. Rep.*, 2012, **30**(1), 108–160, DOI: 10.1039/C2NP20085F.

20 M. A. Ortega and W. A. van der Donk, New Insights into the Biosynthetic Logic of Ribosomally Synthesized and Post-Translationally Modified Peptide Natural Products, *Cell Chem. Biol.*, 2016, **23**(1), 31–44, DOI: 10.1016/j.chembiol.2015.11.012.

21 A. D. de Araujo, M. Mobli, G. F. King and P. F. Alewood, Cyclization of Peptides by Using Selenolanthionine Bridges, *Angew. Chem., Int. Ed.*, 2012, **51**(41), 10298–10302, DOI: 10.1002/anie.201204229.

22 N. Mazo, I. R. Rahman, C. D. Navo, J. M. Peregrina, J. H. Busto, W. A. van der Donk and G. Jiménez-Osés, Synthesis of Fluorescent Lanthipeptide Cytolysin S Analogues by Late-Stage Sulfamidate Ring Opening, *Org. Lett.*, 2023, **25**(9), 1431–1435, DOI: 10.1021/acs.orglett.3c00122.

23 A. C. Ross, H. Liu, V. R. Pattabiraman and J. C. Vederas, Synthesis of the Lantibiotic Lactocin S Using Peptide Cyclizations on Solid Phase, *J. Am. Chem. Soc.*, 2010, **132**(2), 462–463, DOI: 10.1021/ja9095945.

24 G. J. L. Bernardes, J. M. Chalker, J. C. Errey and B. G. Davis, Facile Conversion of Cysteine and Alkyl Cysteines to Dehydroalanine on Protein Surfaces: Versatile and Switchable Access to Functionalized Proteins, *J. Am. Chem. Soc.*, 2008, **130**(15), 5052–5053, DOI: 10.1021/ja800800p.

25 J. M. Chalker, S. B. Gunnoo, O. Boutureira, S. C. Gerstberger, M. Fernández-González, G. J. L. Bernardes, L. Griffin, H. Hailu, C. J. Schofield and B. G. Davis, Methods for Converting Cysteine to Dehydroalanine on Peptides and Proteins, *Chem. Sci.*, 2011, **2**(9), 1666–1676, DOI: 10.1039/C1SC00185J.

26 S. Y. Yap, T. Butcher, R. J. Spears, C. McMahon, I. A. Thanasi, J. R. Baker and V. Chudasama, Chemo- and Regio-Selective Differential Modification of Native Cysteines on an Antibody via the Use of Dehydroalanine Forming Reagents, *Chem. Sci.*, 2024, **15**(22), 8557–8568, DOI: 10.1039/D4SC00392F.

27 J. M. Chalker, L. Lercher, N. R. Rose, C. J. Schofield and B. G. Davis, Conversion of Cysteine into Dehydroalanine Enables Access to Synthetic Histones Bearing Diverse Post-Translational Modifications, *Angew. Chem., Int. Ed.*, 2012, **51**(8), 1835–1839, DOI: 10.1002/anie.201106432.

28 J. Dadová, K.-J. Wu, P. G. Isenegger, J. C. Errey, G. J. L. Bernardes, J. M. Chalker, L. Raich, C. Rovira and

B. G. Davis, Precise Probing of Residue Roles by Post-Translational β,γ-C,N Aza-Michael Mutagenesis in Enzyme Active Sites, *ACS Cent. Sci.*, 2017, **3**(11), 1168–1173, DOI: 10.1021/acscentsci.7b00341.

29 M. S. Messina and H. D. Maynard, Modification of Proteins Using Olefin Metathesis, *Mater. Chem. Front.*, 2020, **4**(4), 1040–1051, DOI: 10.1039/C9QM00494G.

30 L. Zhang and J. P. Tam, Thiazolidine Formation as a General and Site-Specific Conjugation Method for Synthetic Peptides and Proteins, *Anal. Biochem.*, 1996, **233**(1), 87–93, DOI: 10.1006/abio.1996.0011.

31 H. Faustino, M. J. S. A. Silva, L. F. Veiros, G. J. L. Bernardes and P. M. P. Gois, Iminoboronates Are Efficient Intermediates for Selective, Rapid and Reversible N-Terminal Cysteine Functionalisation, *Chem. Sci.*, 2016, **7**(8), 5052–5058, DOI: 10.1039/C6SC01520D.

32 A. Bandyopadhyay, S. Cambray and J. Gao, Fast and Selective Labeling of N-Terminal Cysteines at Neutral pH via Thiazolidino Boronate Formation, *Chem. Sci.*, 2016, **7**(7), 4589–4593, DOI: 10.1039/C6SC00172F.

33 K. Li, M. A. Kelly and J. Gao, Biocompatible Conjugation of Tris Base to 2-Acetyl and 2-Formyl Phenylboronic Acid, *Org. Biomol. Chem.*, 2019, **17**(24), 5908–5912, DOI: 10.1039/C9OB00726A.

34 M. Zheng, F. Haeffner and J. Gao, N-Terminal Cysteine Mediated Backbone-Side Chain Cyclization for Chemically Enhanced Phage Display, *Chem. Sci.*, 2022, **13**(28), 8349–8354, DOI: 10.1039/D2SC03241D.

35 S. Ng, M. R. Jafari, W. L. Matochko and R. Derda, Quantitative Synthesis of Genetically Encoded Glycopeptide Libraries Displayed on M13 Phage, *ACS Chem. Biol.*, 2012, **7**(9), 1482–1487, DOI: 10.1021/cb300187t.

36 K. Itoh, N. Wakabayashi, Y. Katoh, T. Ishii, K. Igarashi, J. D. Engel and M. Yamamoto, Keap1 Represses Nuclear Activation of Antioxidant Responsive Elements by Nrf2 through Binding to the Amino-Terminal Neh2 Domain, *Genes Dev.*, 1999, **13**(1), 76–86, DOI: 10.1101/gad.13.1.76.

37 S. Dayalan Naidu and A. T. Dinkova-Kostova, KEAP1, a Cysteine-Based Sensor and a Drug Target for the Prevention and Treatment of Chronic Disease, *Open Biol.*, 2020, **10**(6), 200105, DOI: 10.1098/rsob.200105.

38 P. Deshmukh, S. Unni, G. Krishnappa and B. Padmanabhan, The Keap1-Nrf2 Pathway: Promising Therapeutic Target to Counteract ROS-Mediated Damage in Cancers and Neurodegenerative Diseases, *Biophys. Rev.*, 2017, **9**(1), 41–56, DOI: 10.1007/s12551-016-0244-4.

39 S. Bono, M. Feligioni and M. Corbo, Impaired Antioxidant KEAP1-NRF2 System in Amyotrophic Lateral Sclerosis: NRF2 Activation as a Potential Therapeutic Strategy, *Mol. Neurodegener.*, 2021, **16**(1), 71, DOI: 10.1186/s13024-021-00479-8.

40 M. Hammad, M. Raftari, R. Cesário, R. Salma, P. Godoy, S. N. Emami and S. Haghdoost, Roles of Oxidative Stress and Nrf2 Signaling in Pathogenic and Non-Pathogenic Cells: A Possible General Mechanism of Resistance to Therapy, *Antioxidants*, 2023, **12**(7), 1371, DOI: 10.3390/antiox12071371.

41 A. E. Owens, J. A. Iannuzzelli, Y. Gu and R. Fasan, MOrPH-PhD: An Integrated Phage Display Platform for the Discovery of Functional Genetically Encoded Peptide Macrocycles, *ACS Cent. Sci.*, 2020, **6**(3), 368–381, DOI: 10.1021/acscentsci.9b00927.